J Mater Sci: Mater Med (2015) 26:120
DOI 10.1007/s10856-015-5426-2

SPECIAL ISSUE: ESB 2014

Engineering and Nano-engineering Approaches for Medical Devices

Nanoscale neuroelectrode modification via sub-20 nm silicon nanowires through self-assembly of block copolymers

Parvaneh Mokarian-Tabari · Catalina Vallejo-Giraldo · Marc Fernandez-Yague · Cian Cummins · Michael A. Morris · Manus J. P. Biggs

Received: 25 July 2014 / Accepted: 15 September 2014 / Published online: 13 February 2015

Abstract Neuroprosthetic technologies for therapeutic neuromodulation have seen major advances in recent years but these advances have been impeded due to electrode failure or a temporal deterioration in the device recording or electrical stimulation potential. This deterioration is attributed to an intrinsic host tissue response, namely glial scarring or gliosis, which prevents the injured neurons from sprouting, drives neurite processes away from the neuroelectrode and increases signal impedance by increasing the distance between the electrode and its target neurons. To address this problem, there is a clinical need to reduce tissue encapsulation of the electrodes in situ and improve long-term neuroelectrode function. Nanotopographical modification has emerged as a potent methodology for the disruption of protein adsorption and cellular adhesion in vitro. This study investigates the use of block copolymer self-assembly technique for the generation of sub-20 nm nanowire features on silicon substrates. Critically, these nanostructures were observed to significantly reduce electrical impedance and increase conductivity. Human neuroblastoma SH-SY5Y cells cultured on nanowire substrates for up to 14 days were associated with enhanced focal adhesion reinforcement and a reduction in proliferation. We conclude that nanowire surface modulation may offer significant potential as an electrode functionalization strategy.

P. Mokarian-Tabari (✉) · C. Cummins · M. A. Morris
Department of Chemistry, Tyndall National Institute, University College Cork, Cork, Ireland
e-mail: p.mokarian@ucc.ie

P. Mokarian-Tabari · M. A. Morris
Centre for Research on Adaptive Nanostructures and Nanodevices (CRANN) and AMBER Centre, Trinity College Dublin, Dublin, Ireland

C. Vallejo-Giraldo · M. Fernandez-Yague · M. J. P. Biggs (✉)
Network of Excellence for Functional Biomaterials (NFB), National University of Ireland, Galway, Ireland
e-mail: manus.biggs@nuigalway.ie

1 Introduction

The translation of neuroelectrode-based therapies into long-term clinical solutions is problematic due to soft-tissue scarring, and sub-optimal electrode integration [1], which prevents the injured neurons from regenerating, drives neurite processes away from the neuroelectrodes and increases signal impedance. Inert anti-fouling polymers are commonly used to coat the non-stimulating elements of the electrode, however this material act as a potent dielectric barrier and cannot be employed to reduce glial cell adhesion and scarring on the stimulating surface.

Nanotopographically modified neuroelectrode surfaces may provide excellent opportunities for functional modification, through the modulation of both protein adsorption and cell adhesion to promote electrode integration. Further, nanotopography may be employed to significantly enhance electrode performance by reducing the interfacial impedance. The success or failure of novel neuroelectrode systems hinge on an implanted electrode system that reduces adverse peri-implant encapsulation, reduces neural loss, and receive/target stimulating electrical pulses to from/to the site of interest to achieve maximum therapeutic efficacy.

Highly ordered micro and nanotopographies (<100 nm) have recently been identified as useful in modulating cell adhesion and differentiation [2]. However, a paradigm of nanobiomimetic design is that features with dimensions similar to those of surface bound proteins ($\sim$10 nm) can significantly affect protein adsorption and cellular activity

[3, 4]. Cost effective methodologies for the fabrication of sub-20 nm features are critical for the translation of true nanotechnologies into the clinic, and high-throughput photolithography approaches are rapidly approaching their resolution limitations. Here, we describe a self-assembly process for the production of hexagonally arranged arrays of 20 nm vertical silicon nanowires using a block copolymer, reactive ion etching process and discuss the effect of the surface modifications on cell adhesion and electrical charge transfer in vitro.

2 Results and discussion

2.1 Physicochemical characterisation of silicon substrates

Here we describe the fabrication of sub-20 nm nanowire features in silicon using a block copolymer mask technique. Critically, these nanowire substrates were observed to significantly reduce in the magnitude of electrode impedance due to a significant increase in surface area. Furthermore, preliminary biological observations offer significant insight into the development of next-generation neuroelectrode design.

We used PS-*b*-PEO poly (styrene-*b*-ethylene oxide) block copolymer to make 50 nm thick, nanopatterned, thin films on silicon substrates [5]. The films were exposed to toluene vapor at 50 °C, a common technique known as solvent vapor annealing employed to induce nanophase separation of BCP thin films [6]. Due to the affinity of both polymers with toluene, the chains become mobilised. The phase separation is driven by immiscibility of the two polymer blocks and an ordered dot pattern of hexagonally phase separated polymer is formed (Fig. 1a). The dark dot domains in (Fig. 1a) are PEO and the matrix polymer is composed of PS. To be able to use this pattern as a mask template on silicon, it is necessary to increase the etch contrast between the polymer and the substrate. This was done by an iron oxide inclusion technique [7].

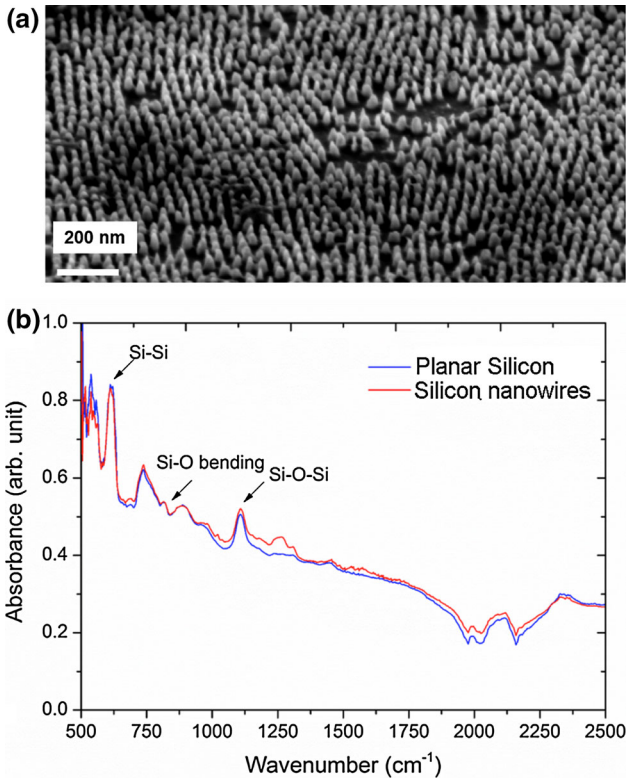

Fig. 2 Si nanowires characterisations. **a** SEM tilted image (~40°) of Si nanowires after pattern transfer of iron oxide dot domain (shown in **c**) to Si substrate following 10 s SiO_2 etch (C_4F_8/H_2) + 90 s Si etch (C_4F_8/SF_6) in ICP/RIE. **b** FT-IR spectra of plain Si and Si nanowire substrate confirms similar surface chemistry

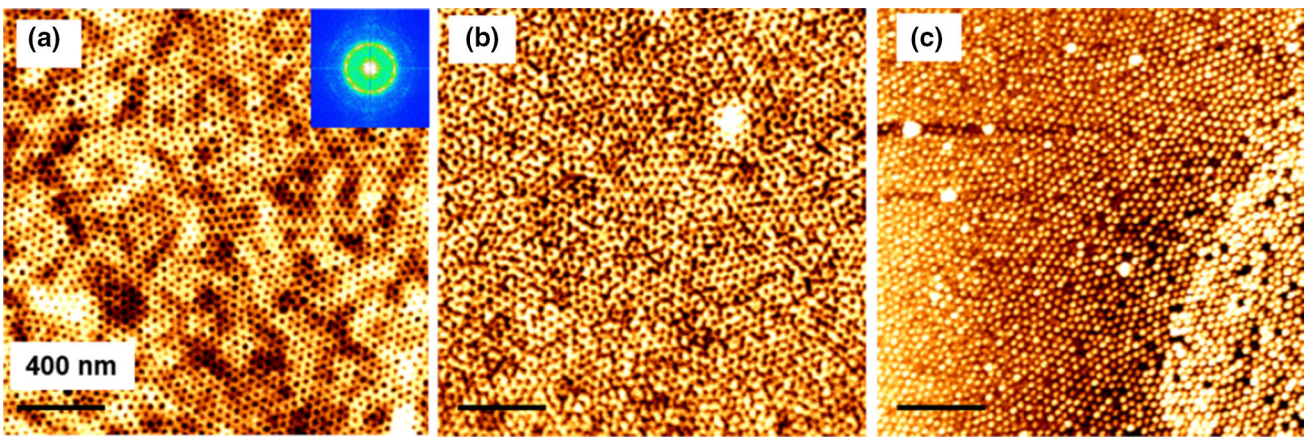

Fig. 1 Block copolymer nanolithography. **a** AFM topographic images of PS-*b*-PEO after annealing. The FFT image indicating a periodicity of 38 nm. **b** After iron oxide inclusion to PEO (*dark domains*) to enhance the etch contrast. **c** After UV/Ozone exposure to remove the matrix polymer (PS) and oxidise the precursor. The *white domains* are iron oxide arrays

After immersing the sample in ethanol for 6 h, an iron nitride III solution was spin cast on PS-*b*-PEO film. The iron nitride immigrates to PEO domains selectively (Fig. 1b). Further exposure of the sample to UV/ozone leads to oxidation of the domains and also removal of most of the PS matrix (Fig. 1c). The template is then etched using an ICP-RIE plasma reactor. Due to the high etch contrast of iron oxide with silicon, we were able to fabricate high aspect ratio vertical nanowires in silicon. Figure 2a is a 40° tilted SEM image of silicon nanowires after removal of iron oxide. The wires are 20 nm in diameter and 92 ± 11.5 nm in height. With this method it is possible to make high aspect ratio (20:1) vertical nanowires (data not shown). FT-IR spectra shown in (Fig. 2b) provides additional information on the surface chemistry of the substrates and indicates that both planar silicon and the nanopatterned silicon possess identical chemical profiles. Different peaks associated with different bonds are indicated.

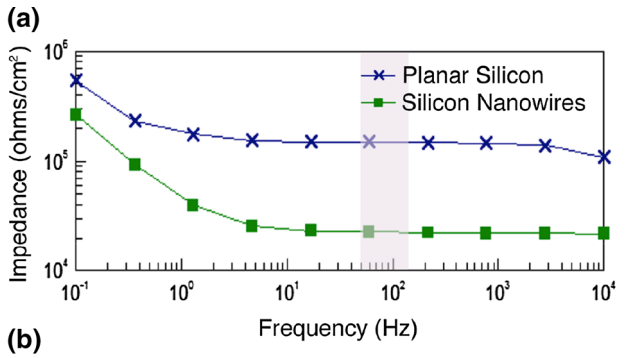

(b)

Substrate	Mean Conductivity (S/cm)	Stardard Desviation
Planar Silicon	1.2	±0.488
Silicon Nanowires	344	±166.5

Fig. 3 Analysis of silicon electrical conductivity. **a** Si nanowire substrates were observed to reduce the electrical impedance relative to planar silicon substrates, assessed at 10^{-1}–10^{4} Hz. The reduction in impedance was particularly significant at physiological relevant frequencies (*shaded*) ($n = 3$). Four-point probe analysis indicated a significant increase in substrate conductivity when patterned with silicon nanowires (**b**)

2.2 Electrical characterisation of silicon substrates

For electrical stimulating devices, increases in electrode impedance can affect current delivery, device battery life, and stimulation thresholds [8–10], with current spinal stimulation systems maintaining functionality for less than 5 years in chronic pain patients due to increased tissue impedance, migration or battery failure [11–14]. Furthermore, the volume of tissue stimulation is dependent on the

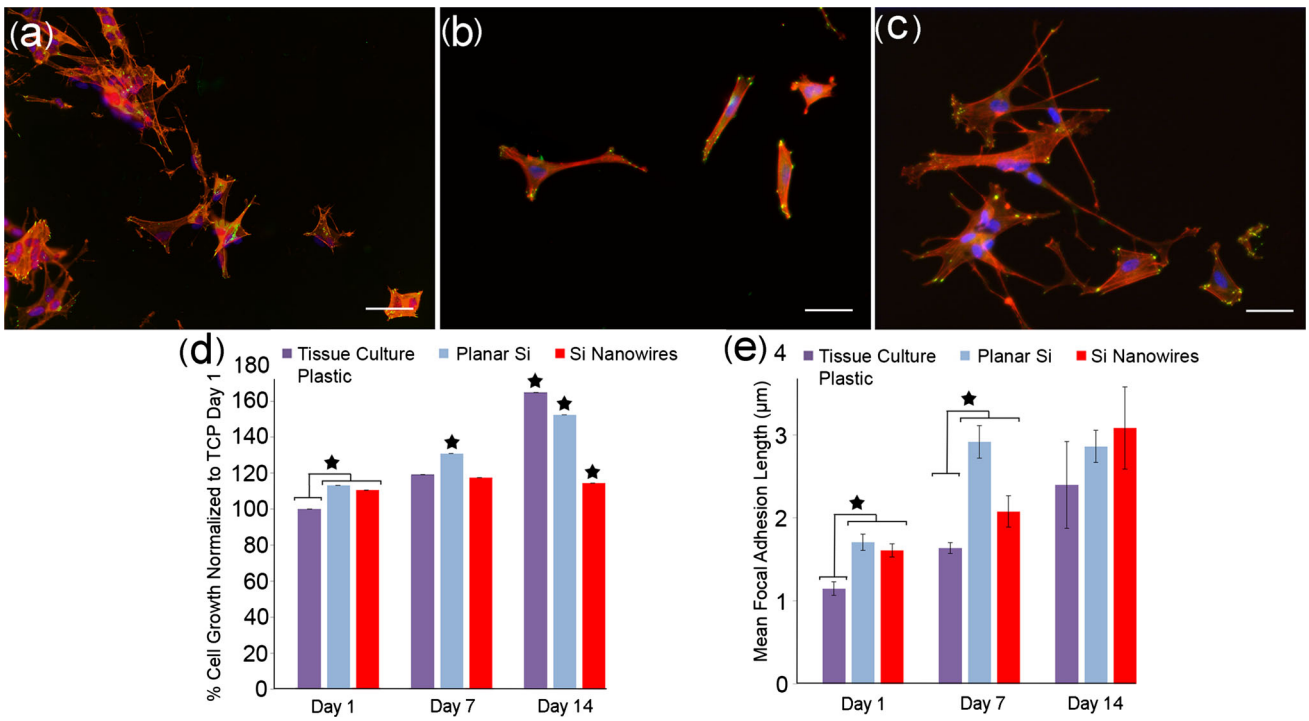

Fig. 4 Human neuroblastoma cell proliferation and adhesion on nanowire substrates. Cells adhered to all experimental substrates. Focal adhesion formation and neurospecific morphology was increased on **c** vertical nanowire substrates relative to **b** planar silicon and **a** control TCP substrates. This was quantified at day analysis of cell proliferation **d** indicated that SH-5YSY cells proliferated on nanowire substrates less efficiently than on planar silicon and control TCP substrates. **e** Nanowire substrates promoted neural cell adhesion through the generation of elongated focal adhesions. *Red* actin, *green* paxillin, *blue* DAPI. *Bar* 50 μm (Color figure online)

electrode–tissue interface impedance when using voltage-controlled stimulation [12, 15].

Electrochemical impedance spectroscopy (EIC) indicated that through surface patterning with nanowire structures the impedance profile of planar silicon can be significantly reduced. In particular, at physiologically relevant electrical frequencies (indicated) this reduction in impedance was by approximately 1 order of magnitude (Fig. 3a). Four-point probe analysis also indicated a significant increase in nanowire substrate conductivity relative to planar silicon substrates (Fig. 3b).

2.3 Cytocompatability of silicon substrates

Human neuroblastoma SH-SY5Y cells were cultured on experimental and control substrates for up to 14 days and assessed for proliferation and adhesion.SH-SY5Y cells were observed to proliferate on control tissue culture plastic (TCP) and planar silicon substrates but not on nanowire substrates as identified by Alamar blue assay. Immunofluorescent labelling of paxillin and subsequent focal adhesion analysis revealed an increase in focal adhesion reinforcement of both planar and silicon nanowire samples, which was present up to day 14 of culture (Fig. 4).

Neurons do not possess a regenerative capacity and hence proliferation at the cell/neuroelectrode interface will be restricted predominantly to the resident glial and migratory leukocyte populations leading to frustrated phagocytosis, local inflammation and neuron death. Although glial cell adhesion was not assessed in this study, it is interesting to suggest that anti-proliferative surfaces may reduce glial proliferation and subsequent gliosis whilst maintaining intimate contact with interfacial neurites through the promotion of focal adhesion reinforcement.

3 Conclusion

The limited success of long-term spinal stimulation is due to the absence of an innovative anti-scaring system that can promote electrode interaction, reduce encapsulation and improve the therapeutic charge transfer to neural tissue. Reactive tissue and consolidated scar tissue have higher resistive properties than normal tissue [15, 16] and changes in electrode impedance can alter the performance of implantable devices. To address this problem, there is a clinical need to reduce scar-tissue encapsulation in situ and improve long-term neuroelectrode function. It can be hypothesised that the chronic performance of neural interfaces can be enhanced by promoting neuron adhesion to the electrode surface to increase device integration and reduce scar tissue encapsulation. Here vertical silicon nanowire substrates fabricated via block copolymer templating were evaluated as potent modulators of cellular adhesion and proliferation and significantly improved the material electrical conductivity.

4 Experimental methods

4.1 Sub-20 nm nanowire fabrication

Polystyrene-*b*- ethylene oxide (PS-b-PEO) diblock copolymer with average molecular masses of blocks $M_{PS} = 42$ kg mol^{-1} and $M_{PEO} = 11$ kg mol^{-1} and PDI (polydispersity index) of 1.07 was purchased from Polymer Source. A 1 wt% solution of polymer in toluene was prepared. The thin film was spin cast at 2,000 r.p.m. on a *p*-type silicon substrate with a 2 nm native oxide layer on top and annealed at 50 °C exposed to toluene. For metal oxide inclusion the film was immersed in anhydrous ethanol for 6 h at 40 °C to obtain activated PEO domains. A 0.4 % iron (III) nitrate nonahydrate solution in ethanol was spin cast on the film. The sample was exposed to UV/Ozone for 3 h to oxidize the precursor and remove the polystyrene polymer matrix. The iron oxide mask was pattern transferred to the silicon substrate performing a 10 s silicon oxide etch (to remove the native oxide layer) using a combination of tetrafluorocarbon (C_4F_4) and hydrogen gases and 90 s siliconetch using a combination of sulphur hexafluoride (SF_6) and trifluoromethane (CHF_3) gases in an (ICP-RIE) inductively coupled plasma-reactive ion etch machine [17].The iron oxide was removes by immersion the patterned substrate in a 10 wt% oxalic acid in water solution for 3 h. Surface morphologies were imaged by scanning probe microscopy in tapping mode and scanning electron microscopy. FT-IR was used to characterise the chemistry of the plain silicon and nanotopography pattern silicon surfaces to make sure the chemistry of the both surfaces are similar.

4.2 Electrical conductivity measurements

Resistance of the films was measured using a four-point probe technique on a custom built apparatus. Four locations on the polymeric film were measured in an area of 2 cm^2.

Electrical impedance spectroscopy (EIS) was performed using a Solartron Instruments controlled by the Z view software with a three electrode set up in a-physiological saline electrolyte buffered with carbonate and phosphate as described in [18]. An AC sine wave of 40 mV amplitude was applied with 0 V DC offset. The impedance magnitude and phase angle were calculated at 1, 10, 100, 1,000, 10,000 Hz [1].

4.3 Cell studies

The human neuroblastoma SH-SY5Y cells were cultured in Dulbeccos modified eagles medium (DMEM), F12 medium and supplemented with 10 % fetal bovine serum and 1 % penicillin/streptomycin (FBS) and all-trans retinoic acid at a final concentration of 10 μM for differentiation into neuronal cell morphology. Cells were seeded onto experimental substrates at a final density of 50,000 cells/cm^2. AlamarBlue® Assay (Life Technologies, UK) was carried out after 1, 7 and 14 days on each of the samples according to manufacturer guidelines and absorbance was measured at 544 excitation and 590 emission wave lengths using a Thermo Scientific Varios-Kan Flash microplate reader.

Cell cultures were fixed in 4 % paraformaldehyde and 1 % sucrose at days, 1, 7 and 14. Indirect immunofluorescent labelling of paxillin was performed as described previously [19]. The samples were subsequently imaged with an Olympus IX 81 fluorescence microscope.

At least 20 randomly selected images at 20× magnification were taken from each tested groups and control groups. The total number of focal adhesion points per cell and their length was directly counted and measured with ImageJ software (National Institutes of Health, USA). All data presented here was confirmed at least using three replicates for each of the tested groups and control groups. The results are expressed as the mean of the values ± standard error. One way ANOVA followed by Bonferroni test were performed to determine the statistical significance ($P < 0.05$), unless otherwise stated.

Acknowledgments The authors would like to acknowledge (AMBER) Advanced Materials and BioEngineering Research and (SFI) Science Foundation Ireland for funding through SFI-AMBER (Grant No. SFI 12/RC/2278 AMBER). We acknowledge the joint funding received from Irish Research Council through IRC New Foundation Scheme/Nano Surface project. Also the authors thank Advance Microscopy Laboratory (AML)/CRANN for their collaboration and facilities. Bell Labs Ireland thanks the Industrial Development Agency (IDA) Ireland for their financial support. M. J. Biggs is a Science Foundation Ireland, Starting Investigator SIRG COFUND fellow, Grant No. 11/SIRG/B2135.

References

1. Green RA, Lovell NH, Wallace GG, Poole-Warren LA. Conducting polymers for neural interfaces: challenges in developing an effective long-term implant. Biomaterials. 2008;29:3393–9.
2. Dalby MJ, Gadegaard N, Tare R, Andar A, Riehle MO, Herzyk P, et al. The control of human mesenchymal cell differentiation using nanoscale symmetry and disorder. Nat Mater. 2007;6:997–1003.
3. Hammarin G, Persson H, Dabkowska AP, Prinz CN. Enhanced laminin adsorption on nanowires compared to flat surfaces. Colloids Surf B. 2014;122C:85–9.
4. Kam KR, Walsh LA, Bock SM, Ollerenshaw JD, Ross RF, Desai TA. The effect of nanotopography on modulating protein adsorption and the fibrotic response. Tissue Eng Part A. 2014;20:130–8.
5. Mokarian-Tabari P, Collins TW, Holmes JD, Morris MA. Cyclical "Flipping" of morphology in block copolymer thin films. ACS Nano. 2011;5:4617–23.
6. Sinturel C, Vayer M, Morris M, Hillmyer MA. Solvent vapor annealing of block polymer thin films. Macromolecules. 2013;46:5399–415.
7. Ghoshal T, Maity T, Godsell JF, Roy S, Morris MA. Large scale monodisperse hexagonal arrays of superparamagnetic iron oxides nanodots: a facile block copolymer inclusion method. Adv Mater. 2012;24:2390–7.
8. Johnson MD, Otto KJ, Kipke DR. Repeated voltage biasing improves unit recordings by reducing resistive tissue impedances. IEEE Trans Neural Syst Rehabil Eng. 2005;13:160–5.
9. Dorman MF, Smith LM, Dankowski K, McCandless G, Parkin JL. Long-term measures of electrode impedance and auditory thresholds for the Ineraid cochlear implant. J Speech Hear Res. 1992;35:1126–30.
10. De Ceulaer G, Johnson S, Yperman M, Daemers K, Offeciers FE, O'Donoghue GM, et al. Long-term evaluation of the effect of intracochlear steroid deposition on electrode impedance in cochlear implant patients. Otol Neurotol. 2003;24:769–74.
11. Fakhar K, Hastings E, Butson CR, Foote KD, Zeilman P, Okun MS. Management of deep brain stimulator battery failure: battery estimators, charge density, and importance of clinical symptoms. PLoS One. 2013;8:e58665.
12. Butson CR, Maks CB, McIntyre CC. Sources and effects of electrode impedance during deep brain stimulation. Clin Neurophysiol. 2006;117:447–54.
13. Kay AD, McIntyre MD, Macrae WA, Varma TR. Spinal cord stimulation—a long-term evaluation in patients with chronic pain. Br J Neurosurg. 2001;15:335–41.
14. Quigley DG, Arnold J, Eldridge PR, Cameron H, McIvor K, Miles JB, et al. Long-term outcome of spinal cord stimulation and hardware complications. Stereotact Funct Neurosurg. 2003;81:50–6.
15. Wei XF, Grill WM. Current density distributions, field distributions and impedance analysis of segmented deep brain stimulation electrodes. J Neural Eng. 2005;2:139–47.
16. Williams JC, Hippensteel JA, Dilgen J, Shain W, Kipke DR. Complex impedance spectroscopy for monitoring tissue responses to inserted neural implants. J Neural Eng. 2007;4:410–23.
17. Borah D, Shaw MT, Rasappa S, Farrell RA, O'Mahony C, Faulkner CM, et al. Plasma etch technologies for the development of ultra-small feature size transistor devices. J Phys D. 2011;44:12.
18. Wei XF, Grill WM. Impedance characteristics of deep brain stimulation electrodes in vitro and in vivo. J Neural Eng. 2009;6:046008.
19. Biggs MJ, Capdevila EP, Vallejo-Giraldo G, Wind S. Cellular response to ferroelectric PVDF-TrFE nanoscale surfaces formed by varying polymer concentration. Pharm Nanotechnol. 2014;2:42–8.